RSC Advances

PAPER

View Article Online
View Journal | View Issue

Cite this: *RSC Adv.*, 2015, **5**, 6259

Preparation of Co–N–C supported on silica spheres with high catalytic performance for ethylbenzene oxidation†

Zhigang Liu,*[a] Lintao Ji,[a] Xulong Dong,[a] Zhen Li,[b] Lingling Fu[a] and Qiuan Wang[a]

Received 9th September 2014
Accepted 17th December 2014

DOI: 10.1039/c4ra09269d

www.rsc.org/advances

In this study, Co–N–C supported on silica spheres is prepared through heat-treatment of supported metalloporphyrin in an N_2 atmosphere. The catalytic performance of the catalysts for ethylbenzene oxidation is investigated and these catalysts are characterized by techniques such as BET, FT-IR, UV-vis, TEM and XPS. In comparison with other catalysts such as supported cobalt porphyrin and unsupported cobalt porphyrin, Co–N–C supported on silica spheres shows much higher catalytic activity for ethylbenzene oxidation (15.7%) and selectivity to acetophenone (76.5%). In addition, the catalyst can retain its high catalytic activity after several reuses. The results show that the high catalytic performance of the catalyst may be attributed to the formation of Co–N_4–C sites during the heat-treatment and supported Co–N–C catalysts may be beneficial to yield more Co–N_4–C sites.

1. Introduction

Metalloporphyrins, well known for their high performance in many biological functions, have attracted lots of attention in the last few decades, because they can be employed to mimic natural enzymes as active reaction sites.[1–3] However, the direct application of metalloporphyrins faces challenge due to the formation of catalytically inactive dimmers and/or self-destruction in some oxidizing reactions.[4,5] Moreover, recovering of homogeneous metalloporphyrins is also an unresolved problem. As one promising approach, metalloporphyrins grafted on supports, such as zeolite, silica and carbon materials, are used as an alternative way to protect metalloporphyrins from the above-mentioned drawbacks.[6–9] However, this practice inevitably leads to dilution of active sites and difficult diffusion of substrates, which results in lowering activity of supported catalysts. Furthermore, supported metalloporphyrins are also suffering from thermal decomposition and self destruction in comparably high reaction temperature.[10]

However, heat-treatment of metalloporphyrins has been proved to be an effective way to improve the catalytic performance of catalysts. In these reports,[11–14] it is discovered that M–N–C is formed and acts as the active sites. Wang *et al.*[15] has proposed that N plays a significant effect in improving the electrocatalytic activity. They describe that the nitrogen atoms have the electron-accepting ability in nitrogen-doped graphene (N-graphene). In addition, this class of catalyst normally shows inertness to alcohol oxidation in the oxygen reduction reaction (*i.e.* ORR).[16]

In this study, we develop a kind of catalysts (*i.e.* Co–N–C/SN) for ethylbenzene oxidation through heat-treatment of supported metalloporphyrin in N_2 atmosphere. However, heat-treatment may alter the integrity of adsorbed metalloporphyrin compounds and this makes it more difficult to identify the nature of the catalytic active site for ethylbenzene oxidation. Hereafter, comprehensive characterization techniques such as FT-IR, UV-vis, TEM and XPS have been used to discover the relationship between the structural properties and the catalytic performance of the catalysts.

2. Experimental

2.1. Preparation of the catalysts

2.1.1. Synthesis of cobalt(II) 5-(4-carboxyphenyl)-10,15,20-triphenyl porphyrin (CoTPP). The compound is synthesized as described in literature.[17] Typically, 4.69 g of pyrrole is added dropwise into a three-neck flask loading a mixture of 250 ml propanoic acid, 5.56 g benzaldehyde and 2.62 g 4-carboxy benzaldehyde, and then heated to reflux for 30 min. The resultant product is cooled overnight, then filtered and purified. 5-(4-Carboxyphenyl)-10,15,20-triphenyl porphyrin is obtained. 1.0 g of the obtained porphyrin is dissolved in 100 ml *N*,*N*-dimethylformamide (DMF). Following that, after 2.54 g of $CoCl_2 \cdot 6H_2O$ is loaded, the mixture is heated to reflux under stirring until porphyrin is exhausted. Cooling overnight, the solution is filtered and washed repeatedly with hot water, and

[a]*School of Chemistry and Chemical Engineering, Hunan University, Changsha, Hunan, 410082, China. E-mail: liuzhigang@hnu.edu.cn; Tel: +86-731-8882-3327*

[b]*Australian Institute of Innovative Materials, University of Wollongong, Innovation Campus, North Wollongong, NSW 2500, Australia*

† Electronic supplementary information (ESI) available. See DOI: 10.1039/c4ra09269d

the obtained product is denoted as CoTPP. The heated product is assigned as Co–N–C.

2.1.2. Synthesis of modified SiO_2 solid spheres. SiO_2 solid spheres are prepared using a modified Stöber process.[18,19] In a typical synthesis, 4.5 ml tetraethyl orthosilicate (TEOS) is rapidly added into a mixture of 61.7 ml ethanol, 24.7 ml H_2O, and 9.0 ml ammonium. The mixture is vigorously stirred at room temperature for 24 h and then filtered, washed and dried. Following after that, 0.90 g of as-prepared SiO_2, 12 ml 3-aminopropyltrimethoxysilane (APTES) and 30 ml methylbenzene are loaded and heated to reflux for 24 h. The achieved white solid is filtered and washed with methylbenzene and ethanol and then dried under vacuum. The obtained product is denoted as SN.

2.1.3. Synthesis of CoTPP immobilized on SN. 0.010 g CoTPP, 0.100 g SN and 20 ml of dichloromethane (DCM) are loaded into a three-neck flask, and then heated to reflux for 24 h. The resultant is washed in DCM and ethanol, respectively, following separation by centrifugation and then dried in a vacuum oven at 80 °C overnight. The obtained product is denoted as CoTPP/SN. Following that, the dried catalyst is heated at 800 °C for 1 h with a heat rate of 20 °C min^{-1} in N_2 atmosphere according to literatures.[11–14] The product is assigned as Co–N–C/SN.

Similarly, when Co, *i.e.* $CoCl_2 \cdot 6H_2O$, is immobilized on SN with an identical molar ratio as mentioned in Co–N–C/SN, and the product is designated as Co/SN. The specific surface area of Co–N–C/SN is 15.1 m^2 g^{-1} and CoTPP loading in CoTPP/SN is 9.2 mg $g_{\text{-cat}}^{-1}$.

2.2. Characterization of the catalysts

Surface area was measured by nitrogen adsorption/desorption at −196 °C on an Autosorb-6b apparatus from Quanta Chrome Instruments. The samples were degassed at 160 °C for 2 h prior to the adsorption experiments. X-ray diffraction patterns are obtained using CuKα radiation (50 kV and 10 mA, Japan D2IIIB diffractometer). FT-IR spectra were carried out on a Vertex 70 (Bruker) Fourier transform infrared spectrophotometer. UV-vis diffuse reflectance spectra of solid samples were collected on the Shimadzu 2450 spectrophotometer. The morphology of samples was measured by a transmission electron microscopy (TEM, JEM-2100F) with an electron microscope operating at an 80 kV voltage. X-ray photoelectron spectroscopy (XPS) measurements were performed with a RBD upgraded PHI-5000C ESCA system (Perkin Elmer) with Mg Kα radiation ($h\nu$ = 1253.6 eV) or Al Kα radiation ($h\nu$ = 1486.6 eV). The obtained binding energies were calibrated using the C1s peak at 284.6 eV as the reference.

2.3. Catalytic activity

The catalytic performance of the catalysts is measured in a 50 ml autoclave for solvent-free oxidation of ethylbenzene with a magnetic stirrer. 10 ml of ethylbenzene and 30 mg catalyst are loaded into the reactor. Then the reactor is sealed and kept at 8.0 atm with pure O_2. The reaction temperature is kept at 120 °C for 5 h. The sample is analyzed by gas chromatography (a Shimadzu GC-2014 equipped with a capillary column (RTX-5, 30 m Ø 0.25 mm) using a flame ionization detector) with internal standard method using bromobenzene and 1,4-dichlorobenzene as reference. The catalyst is recovered by centrifugation, then washed with ethanol and dried at 80 °C for 12 h.

3. Results and discussion

3.1. Catalytic performance

The catalytic performance of SN, Co–N–C, Co/SN, Co–N–C/SN and blank (or called as autocatalysis system) for ethylbenzene oxidation is displayed in Table 1. 15.7% of ethylbenzene conversion over Co–N–C/SN is achieved, much higher than those over other catalysts. The blank has the ethylbenzene conversion of 4.3%, while the ethylbenzene conversion over SN is only 3.5%. Obviously, the addition of SN may depress the ethylbenzene conversion. As for Co–N–C, ethylbenzene conversion reaches 7.0%. When Co–N–C is supported on SN and Co–N–C/SN is prepared, the ethylbenzene conversion over Co–N–C/SN is 15.7%. Likewise, Co is supported on SN and Co/SN is achieved, the ethylbenzene conversion over Co/SN is 6.2%. In addition, Co–N–C/SN also shows comparable higher selectivity to acetophenone than SN, Co–N–C, Co/SN and blank (*i.e.*, 76.5% *vs.* 63.9%, 66.7%, 68.3% and 59.0%).

Apparently, in comparison with SN, Co–N–C, Co/SN and blank, Co–N–C/SN displays relatively higher ethylbenzene conversion and selectivity to acetophenone. As shown in Table 1, the surface area and pore volume of Co–N–C/SN are both much smaller than those of SN and Co–N–C, and similar to those of Co/SN. Combined with the catalytic performance of the corresponding catalysts, it can be deduced that surface areas may not play a key role in the catalytic performance of the catalysts for ethylbenzene oxidation. Furthermore, though Co/SN and Co–N–C/SN possess almost similar surface areas and cobalt content, a much higher catalytic activity is achieved over Co–N–C/SN than Co/SN. This may be due to the appearance of Co–N–C sites in Co–N–C/SN.[20]

The reusability of Co–N–C/SN for ethylbenzene oxidation is also investigated. The recovered catalyst is washed several times with ethanol to remove residues and dried at 80 °C for 12 h. Following that, the catalyst is reused for ethylbenzene oxidation. As shown in Fig. 1, Co–N–C/SN remains comparably active even at the third reuse with 14.2% of ethylbenzene conversion and 71.1% of selectivity to acetophenone, which is similar to the result in the first run (*i.e.*, 15.7% of ethylbenzene conversion and 76.5% of selectivity to acetophenone).

3.2. FT-IR

FT-IR spectroscopy is generally used to characterize the fine structure of samples. As shown in Fig. 2, the absorption bands around 3400 cm^{-1} are ascribed to the adsorbed water.[21–23] Bands located at 1101 cm^{-1}, 945 cm^{-1}, 802 cm^{-1} and 476 cm^{-1} are associated with the Si–O–Si asymmetric bond stretching vibration, the Si–OH stretching vibration, and the network Si–O–Si symmetric bond stretching vibration, respectively.[24] As for SN, a weak resonance could be found at 1535 cm^{-1} which

Table 1 Catalytic performance of the catalysts for ethylbenzene oxidation[a]

Sample	Surface area (m^2 g^{-1})	Pore volume (ml g^{-1})	Conversion (%)	Selectivity (%)	
				Acetophenone	Phenethyl alcohol
SN	30.8	0.092	3.5	63.9	30.6
Co–N–C	53.6	0.119	7.0	66.7	28.2
Co/SN	15.4	0.044	6.2	68.3	31.7
Co–N–C/SN	15.1	0.043	15.7	76.5	21.3
Blank	—	—	4.3	59.0	34.9

[a] Reaction conditions: catalyst 30 mg, ethylbenzene 10 ml, O_2 pressure 8.0 atm, temperature 120 °C, and reaction time 5 h.

Fig. 1 The reusability of Co–N–C/SN. Reaction conditions: catalyst 30 mg, ethylbenzene 10 ml, O_2 pressure 8.0 atm, temperature 120 °C, and reaction time 5 h.

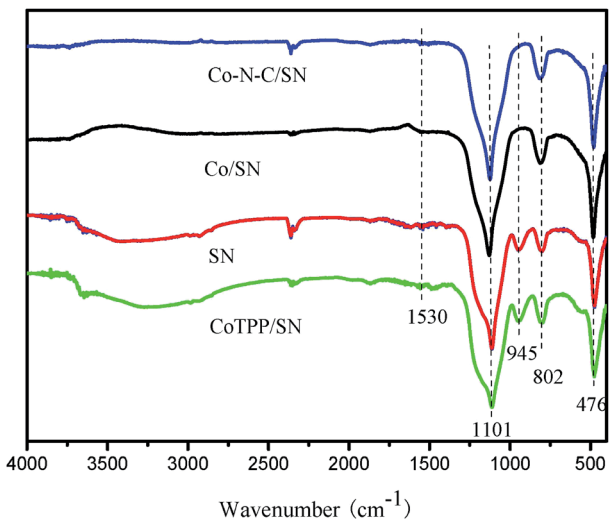

Fig. 2 FT-IR spectra of Co–N–C/SN, Co/SN, SN and CoTPP/SN.

corresponds to the bands of the N–H group vibration on the surface of silica modified with APTES.[25] Normally, amide bonds are supposed to form in CoTPP/SN and the peak at 1535 cm^{-1} is ascribed to the formation of N–H group in amide bonds. However, the resonance in CoTPP/SN is remarkable feeble, compared with the bands of Si–OH groups. This may assigned to the low content of metalloporphyrin in CoTPP/SN (*i.e.*, 9.2 mg $g_{\text{-cat}}^{-1}$) and the signal of amide bonds is beyond the sensitivity of the instrument. However, it is more reasonable to deduce that metalloporphyrin is physically absorbed on the surface of SN and the supposed amide bonds never come into form.

However, if heated at 800 °C, the bands of N–H groups in Co/SN and Co–N–C/SN have disappeared. Apparently, these groups must have been destroyed and carbonized when treated at 800 °C in N_2 atmosphere. Moreover, the bands of Si–OH groups at 945 cm^{-1}, as for Co/SN and Co–N–C/SN, could not be found. This further verifies that heat-treatment has caused broken some chemical bonds and destroyed groups such as Si–OH, N–H and metalloporphyrin rings.

3.3. UV-vis

The UV-vis spectra of CoTPP, CoTPP/SN, Co–N–C/SN and Co–N–C are illustrated in Fig. 3. With respect to CoTPP, the bands at 428 nm and 545 nm are ascribed to Soret bands and Q bands, respectively. These are the characteristic UV-vis peaks of porphyrin rings.[25,26] The similar peaks can also be found in the spectrum of CoTPP/SN, indicating that the porphyrin rings in

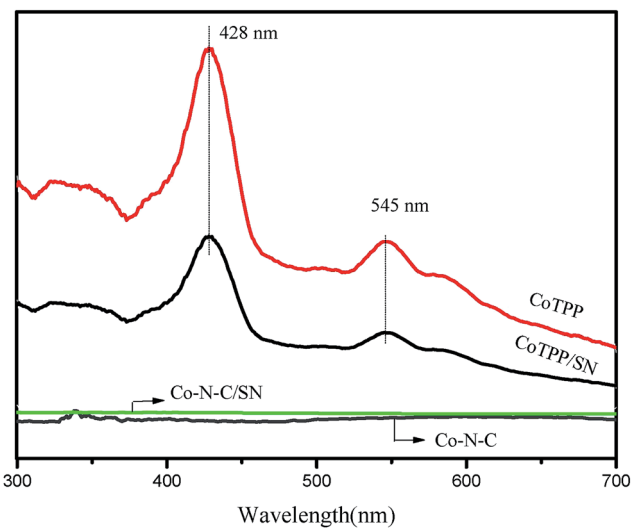

Fig. 3 UV-vis spectra of CoTPP, CoTPP/SN, Co–N–C/SN and Co–N–C.

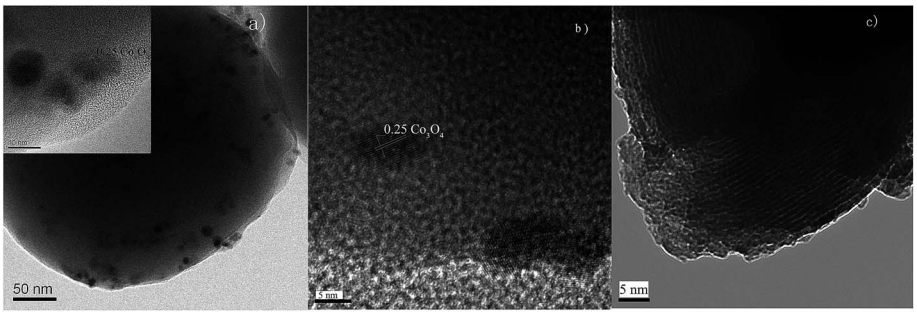

Fig. 4 TEM images of (a) CoTPP/SN; (b) Co–N–C/SN; (c) Co–N–C.

CoTPP/SN are not decomposed when metalloporphyrin is anchored onto SN. Typically, a slight blueshift in the Soret bands, as for the supported metalloporphyrin, is observed compared to their homogeneous counterpart due to the interactions between the porphyrin and SN.[17,27] Nevertheless, when CoTPP and CoTPP/SN are heated at 800 °C in N_2 atmosphere, Co–N–C/SN and Co–N–C are achieved and the heat-treatment may result in the disappearance of Soret bands and Q bands. It is evident that metalloporphyrin rings have decomposed in Co–N–C/SN and Co–N–C, which may lead to the formation of Co–N–C sites.

3.4. TEM

The TEM images of Co/SN, Co–N–C/SN and Co–N–C are illustrated in Fig. 4a–c, respectively. In Fig. 4a, as for Co/SN, cobalt compounds with particle sizes of about 9.5 nm are dispersed on the surface of SN. Likewise, as shown in Fig. 4b, it can be found that cobalt compounds with particle sizes of about 7.0 nm are dispersed on the surface of SN in Co–N–C/SN (as shown in ESI, Fig. S1†). Obviously, CoTPP as precursor may be helpful to hinder the growth of cobalt compound particles on the surface of SN during the heat-treatment. This may be attributed to the formation of graphitic carbon to interrupt the particle sintering.[15] With respect to Co–N–C, as shown in Fig. 4c, graphitic layers can be clearly observed. Generally speaking, carbon materials, as reported in literature,[20] may tightly interact with metal ions when treated at comparably high temperature in N_2 atmosphere.

3.5. XPS

The ratio analysis of the peaks in XPS spectra of the catalysts is listed in Table 2. It can be found that the content of C is the largest part among all surface components except Co/SN. As for Co/SN, the carbon ratio is 31.23%, mainly originating from the carbonization of APTES when heated in N_2 atmosphere. Moreover, the cobalt contents in Co/SN and Co–N–C/SN are very similar, namely, 0.41% and 0.48%, respectively.

The XPS spectra of the catalysts are depicted in Fig. 5a. The Co (2p) spectra for all coverages investigated show that the as-deposited film contained a mixture of Co^{3+} (787.6 eV) and Co^{2+} (and 796.4 eV).[28,29] The peak at 778 eV is ascribed to the presence of Co metallic particles.[30] Moreover, Co–N–C/SN gives the peak at 781.8 ± 0.2 eV, due to the cobalt associated with N in Co–N_x structure.[20]

However, their nitrogen contents are different. The nitrogen content in Co–N–C/SN is up to 1.10%, far larger than that in Co/SN. Obviously, nitrogen must play a significant role in enhancing the catalytic performance of the catalysts for ethylbenzene oxidation. Nevertheless, even though the nitrogen content in Co–N–C is close to that in Co–N–C/SN, Co–N–C/SN has much higher catalytic performance for ethylbenzene oxidation as mentioned above. Therefore, the nitrogen has been analyzed according to the decomposed N_{1s} XPS spectra of the catalysts in Fig. 5b–d. And the four types of nitrogen are pyridine type nitrogen (Pyridinic N, 398.4 eV), pyrrole type nitrogen (Pyrrolic N, 400.0 eV), graphite type nitrogen (Graphitic N, 401.0 eV) and oxidized nitrogen (Oxidized N, 402.6 eV), respectively.[31] As shown in Table 2, in comparison with Co–N–C and Co–N–C/SN, oxidized nitrogen can only been found in Co/SN with the lowest activity (shown in Table 1). It is evident to deduce that oxidized nitrogen is not beneficial to ethylbenzene oxidation. Generally, the electron donating or accepting ability of nitrogen atoms may facilitate the catalytic performance of the metal centers.[15] However, oxygen in oxidized nitrogen exerts an influence on the electron donation or accepting of nitrogen atoms and interrupts this process. As for Co–N–C/SN, there are

Table 2 The ratio analysis of the peaks in XPS spectra of the catalysts

				%N				
Sample	%C	%O	%Co	Total	Pyridinic	Pyrrolic	Graphitic	Oxidized
Co–N–C/SN	64.25	23.00	0.41	1.10	18.5	31.5	27.7	22.3
Co/SN	31.23	46.17	0.48	0.28	0	0	0	100
Co–N–C	79.69	14.52	1.89	1.16	30.0	27.8	24.6	17.6

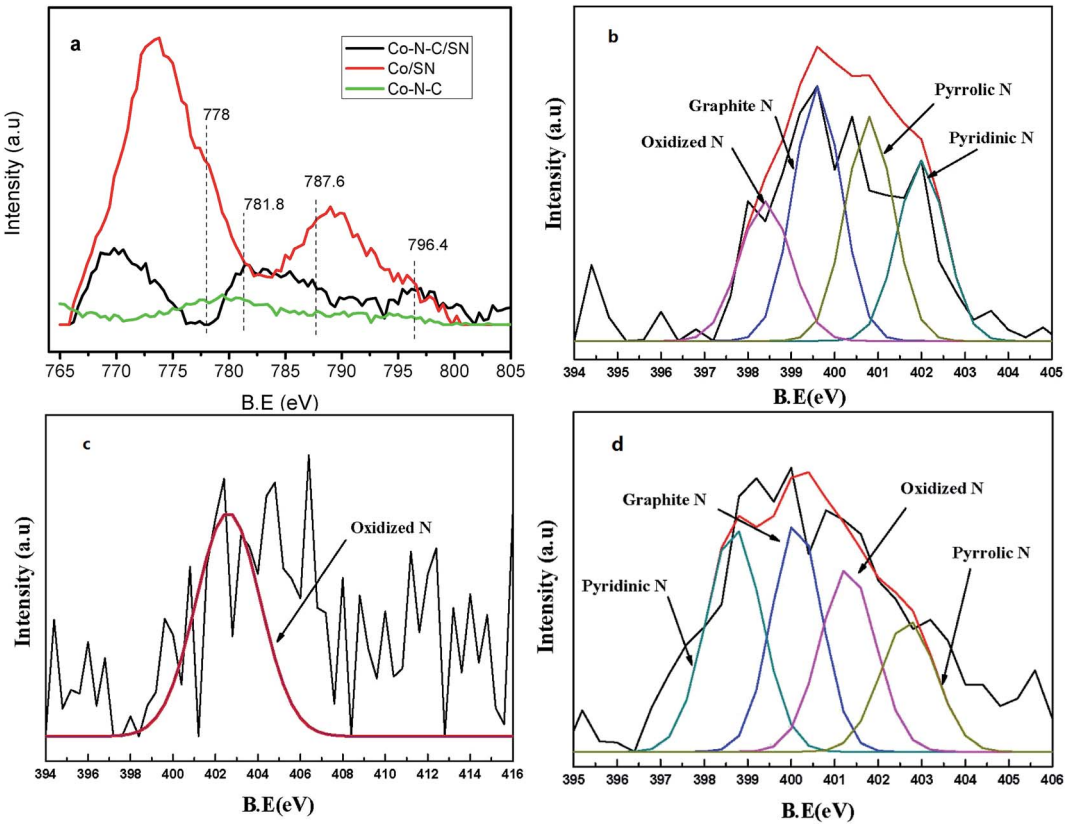

Fig. 5 (a) Co_{2p} XPS spectra of Co–N–C/SN, Co/SN and Co–N–C, (b) decomposed N_{1s} XPS spectra of Co–N–C/SN, (c) decomposed N_{1s} XPS spectra of Co/SN, (d) decomposed N_{1s} XPS spectra of Co–N–C.

more pyrrolic nitrogen than that in Co–N–C, namely, there exists more Co–N_4–C. Combined with the data of catalytic activity in Table 1, more Co–N_4–C sites there are, higher activity the catalysts have. As a result, Co–N_4–C sites in Co–N–C/SN may play an important role in obtaining higher catalytic performance.

4. Conclusions

Compared with other catalysts, Co–N–C/SN shows remarkable high catalytic activity for ethylbenzene oxidation (15.7%) and selectivity to acetophenone (76.5%). Moreover, Co–N–C/SN, in spite of its ability in effective and effortless recovering, can retain its high catalytic activity in the third run. These catalysts are characterized by techniques such as BET, FT-IR, UV-vis, TEM and XPS. The results show that heat-treatment is verified to be necessary for these catalysts to improve their catalytic performance, due to the formation of Co–N_4–C sites during the heat-treatment. In particular, compared with Co–N–C, Co–N–C/SN may have more Co–N_4–C sites, which results in higher catalytic activity for ethylbenzene conversion.

Acknowledgements

The authors gratefully acknowledge the financial support from National Natural Science Foundation of China (no. 21103045, 1210040, 1103312) and the Fundamental Research Funds for the Central Universities.

Notes and references

1 E. M. Davoras and A. G. Coutsolelo, *J. Inorg. Biochem.*, 2003, **94**, 161.
2 C. C. Guo, M. F. Chu and Q. Liu, *Appl. Catal., A*, 2003, **246**, 303.
3 S. Rismayani, M. Fukushima and A. Sawada, *J. Mol. Catal. A: Chem.*, 2004, **217**, 13.
4 K. S. Suslick, P. Bhyrappa, J. H. Chou, M. E. Kosal, S. Nakagaki, D. W. Smithenry and S. R. Wilson, *Acc. Chem. Res.*, 2005, **38**, 283.
5 S. Nakagaki, G. S. Machado, M. Halma, A. A. S. Marangon, K. A. D. F. Castro, N. Mattoso and F. Wypych, *J. Catal.*, 2006, **242**, 110.
6 M. Ghiaci, F. Molaie, M. E. Sedaghat and N. Dorostkar, *Catal. Commun.*, 2010, **11**, 694.
7 D. W. Feng, Z. Y. Gu, J. R. Li, H. L. Jiang, Z. W. Wei and H. C. Zhou, *Angew. Chem.*, 2012, **124**, 10453.
8 X. Guo, D. H. Shen, M. Tian, Q. Liu, C. C. Guo and Z. G. Liu, *J. Mol. Catal. A: Chem.*, 2011, **351**, 174.
9 Z. J. Zhang, L. Wojtas, M. Eddaoudi and M. J. Zaworotko, *J. Am. Chem. Soc.*, 2013, **135**, 5982.

10 D. H. Shen, L. T. Ji, Z. G. Liu, W. B. Sheng and C. C. Guo, *J. Mol. Catal. A: Chem.*, 2013, **379**, 15.
11 H. Alt, H. Binder and G. Sandstede, *J. Catal.*, 1973, **28**, 8.
12 Z. F. Ma, X. Y. Xie, X. X. Ma, D. Y. Zhang, Q. Ren, N. H. Mohr and V. M. Schimidt, *Electrochem. Commun.*, 2006, **8**, 389.
13 J. Liu, S. Y. Bai, Q. R. Jin, C. Li and Q. H. Yang, *Chem. Sci.*, 2012, **3**, 3398.
14 M. Yuasa, A. Yamaguchi, H. Itsuki, K. Tanaka, M. Yamamoto and K. Oyaizu, *Chem. Mater.*, 2005, **17**, 4278.
15 S. Y. Wang, D. S. Yu and L. M. Dai, *J. Am. Chem. Soc.*, 2011, **133**, 5182.
16 X. Wang, M. Waje and Y. Yan, *J. Electrochem. Soc.*, 2004, **151**, A2183.
17 C. X. Liu, Q. Liu and C. C. Guo, *Catal. Lett.*, 2010, **138**, 96.
18 W. Stober, A. Fink and E. J. Bohn, *J. Colloid Interface Sci.*, 1968, **26**, 62.
19 W. Wang, B. H. Gu, L. Y. Liang and W. Hamilton, *J. Phys. Chem. B*, 2003, **107**, 315.
20 K. X. Niu, B. P. Yang, J. F. Cui, J. T. Jin, X. G. Fu, Q. P. Zhao and J. Y. Zhang, *J. Power Sources*, 2013, **243**, 64.
21 K. A. D. F. Castro, A. Bail, P. B. Groszewicz, G. S. Machado, W. H. Schreiner, F. Wypych and S. Nakagaki, *Appl. Catal., A*, 2010, **386**, 51.
22 A. R. McDonald, N. Franssen, G. P. M. Klink and G. Koten, *J. Organomet. Chem.*, 2009, **694**, 2153.
23 H. Yoshino, K. Kamiya and H. Nasu, *J. Non-Cryst. Solids*, 1990, **126**, 68.
24 J. V. Heck and B. G. Christensen, *Tetrahedron Lett.*, 1981, **22**, 5027.
25 G. Huang, T. M. Li and S. Y. Liu, *Appl. Catal., A*, 2009, **371**, 161.
26 W. S. Cho, H. J. Kim, B. J. Littler, M. A. Miller, C. H. Lee and J. S. Lindsey, *J. Org. Chem.*, 1999, **64**, 7890.
27 Y. Zhai, B. Tu and D. Y. Zhao, *J. Mater. Chem.*, 2009, **19**, 131.
28 Z. Ozaydin, S. Yasyerli and G. Dogu, *Ind. Eng. Chem. Res.*, 2008, **47**, 1035.
29 M. E. Bridge and R. M. Lambert, *Surf. Sci.*, 1979, **82**, 413.
30 T. Matsuyama and A. Ignatiev, *Surf. Sci.*, 1981, **102**, 18.
31 A. Morozan, P. Jegou, B. Jousselme and S. Palacin, *Phys. Chem. Chem. Phys.*, 2011, **13**, 21600.

